

# A Detection Method of Cracks and Structural Objects of the Road Surface Image

Naoki Tanaka \*

Chair of Information Systems Eng.  
Kobe University of Mercantile Marine

Masayo MOURI †

Graduate School of Maritime Science and Technology  
Kobe University of Mercantile Marine

## Abstract

This paper introduces a new detection method of crack and structural objects, *whiteline*, *joint* and *manhole* of the road surface image based on morphological technique. Crack and structural objects are difficult to detect directly at the pixel level because of the noise and the vagueness. Some kind of structural information is needed. In the proposed method, we have used morphological operations which are able to extract specify shapes explicitly. Although the method requires the setting of some parameters, it is robust for detecting vague crack and structural objects in the noisy road surface image.

## 1 Introduction

In the maintenance of the road, the detection of crack [1] and structural objects on the road surface, i.e. *white lines* (*center line*), *joint* and *manhole* is one of the major problems. Such objects may be easily recognized by the human visual systems, but are difficult to segment [2]. This difficulty arises from the fact that they cannot be detected directly at the pixel level because of the noise and the vagueness. Some kind of structural information is also needed. We have used morphological operations [3] [4] here to extract specific shapes from the road surface image. For example, in crack detection, the black saddle points are detected via a black top-hat operation [5] with a tiny disk-shaped structure element and in the *whiteline* detection, the large white rectangle regions are extracted via a white top-hat operation with a long line-shaped structure element. An advantage of the proposed method is its robustness against noise and vagueness of the objects.

\* Address: 5-1-1, fukae-minami, higashinada, Kobe 658-0022, Japan. E-mail: tanaka@athena.ti.kshosen.ac.jp

† Address: 5-1-1, fukae-minami, higashinada, Kobe 658-0022, Japan. E-mail: mouri@ti.kshosen.ac.jp

## 2 Notation

### 2.1 Morphological Operation

Mathematical morphology includes four basic operations: dilation, erosion, opening and closing. We make use of these four kind of operations and conditional dilation and top-hat operation throughout this work. The four basic operations are also distinguished into binary operations and gray scale operations, they are denoted as follows:

Dilation( $\oplus, \oplus_g$ ), Erosion( $\ominus, \ominus_g$ ), Opening( $\circ, \circ_g$ ) and Closing( $\bullet, \bullet_g$ ).

Conditional dilation is denoted as follows:

$(G_o(x) |_{\oplus I})$ .

### 2.2 Structure Element

Three kinds of standard shaped structure element, i.e. DISK, LINE and SQUARE are selected in our studying. They are described as following:

- A DISK-shaped structure element with its origin at the center and radius  $i$  is denoted by  $K_{disk}(i)$ .
- A LINE-shaped structure element with length  $l$  and direction  $\theta$  is denoted by  $K_{line\theta}(l)$ .
- A SQUARE-shaped structure element with length of  $e$  is denoted by  $K_{square}(e)$ .

## 3 Crack Detection

The crack detection process falls into four stages: 1) black pixel extraction; 2) saddle point extraction; 3) noise reduction; 4) connecting processing. Let  $G_o(x)$  be a input image, a conditional histogram equalization is adopted in order to improve the contrast of a darker image.

$$H(x) = \begin{cases} HT(G_o(x)) & : Ave(H(x)) \leq 100 \\ G_o(x) & : Ave(H(x)) > 100 \end{cases}$$

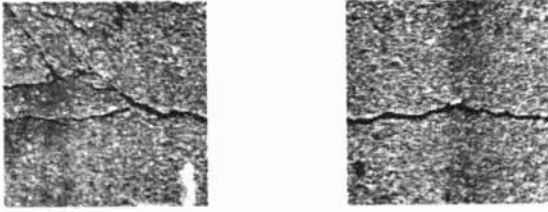


Figure 1:  $H(x)$

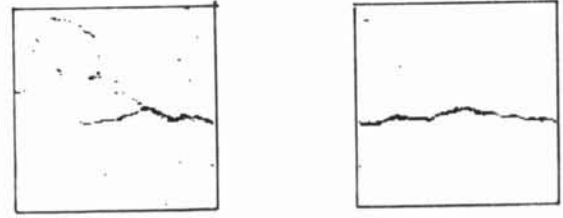


Figure 3:  $T_c(x)$

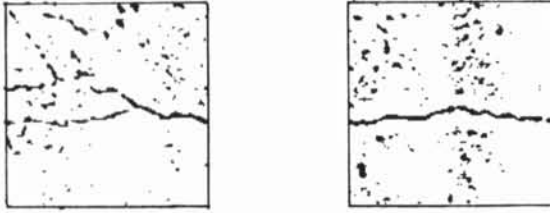


Figure 2:  $B_c(x)$

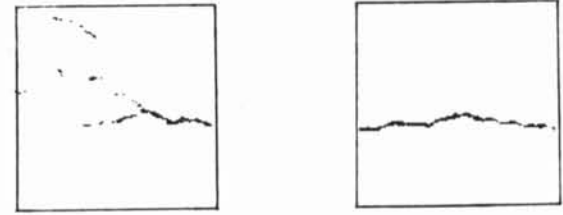


Figure 4:  $M_{c2}(x)$

where  $HT()$  denotes a histogram equalization. An example of histogram equalized image  $H(x)$  is shown in Fig. 1.

### 3.1 Black Region Extraction

Since a crack is constituted by black pixels, black pixel regions are extracted in this stage. To evaluate the relative blackness of the regions, we use the average value  $Ave$  and the standard deviation  $Sd$  of the whole image and local average values  $ave(x)$  and local standard deviations  $sd(x)$  in a window.

$$B_c(x) = \begin{cases} 1 : ((H(x) < (Ave - Sd) \text{ and} \\ (H(x) < (ave(x) - sd(x)) \text{ and } (sd(x) > 20)) \\ 0 : ((H(x) \geq (Ave - Sd) \text{ or} \\ (H(x) \geq (ave(x) - sd(x)) \text{ or } (sd(x) \leq 20)) \end{cases}$$

At this stage, a few large regions and/or a number of small regions are expected to be extracted as crack regions. So,  $B_c(x)$  which includes only a few small regions can be abandoned here. An example of  $B_c(x)$  are shown in Fig. 2.

### 3.2 Saddle point extraction

The saddle point extraction stage is defined as follows.

$$T_c(x) = |HT_{nz}(H(x) \bullet_g K_{disk}(20) - H(x))|_{\theta_1}$$

where  $HT_{nz}()$  denotes a histogram equalization against none zero gray levels, and  $\theta_1 = 230 \sim 255$  which is depend on a value  $Ave(HT(H(x) \bullet_g K_{disk}(20) - H(x)))$ . An example of  $T_c(x)$  are shown in Fig. 3.

### 3.3 Noise Reduction

By taking an intersection of  $B_c(x)$  and  $T_c(x)$ ,  $M_c(x)$  can be obtained.

$$M_c(x) = B_c(x) \cap T_c(x)$$

Eliminating the small regions in  $M_c(x)$ , we can obtain  $M_{c2}(x)$ . An example of  $M_{c2}(x)$  are shown in Fig. 4.

### 3.4 Connecting Processing

Connecting process is starting with the image  $M_c(x)$  and  $M_{c2}(x)$ . To fill gaps of  $M_c(x)$ , a dilation and a conditional dilation are carried out.

$$M_{c3}(x) = M_c(x) \oplus K_{disk}(3)$$

$$M_{c4}(x) = M_{c2}(x) |_{\oplus M_{c3}(x)} \oplus K_{square}(3)$$

Finally the resulting image  $M_{crack}(x)$  can be obtained by eliminating small regions of  $M_{c4}(x)$ . An example of desired image and  $M_{crack}(x)$  are shown in Fig. 5 and Fig. 6 respectively.

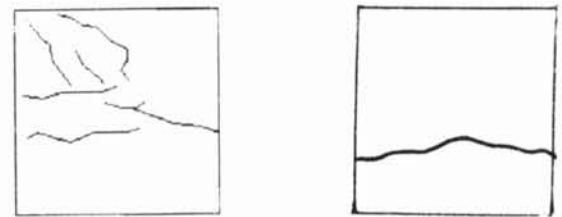


Figure 5: Desired image( $crack$ )

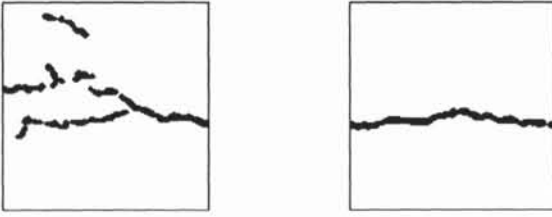


Figure 6:  $M_{crack}$

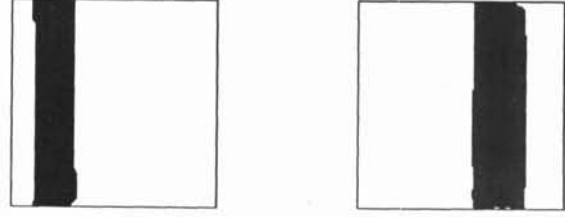


Figure 9:  $T_{white}$



Figure 7:  $G_o(x)(white\ line)$

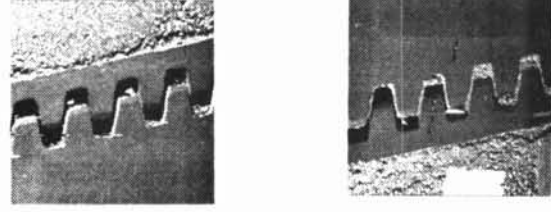


Figure 10:  $G_o(x)(joint)$

#### 4 White Line Detection

Because of the roughness of a road surface , there appear many small gaps and/or holes in *white line* regions of the input image. Therefore a morphological smoothing operation are carried out in order to fill the gaps and the holes.

$$S_w(x) = ((G_o(x) \circ_g K_{disk(7)}) \bullet_g K_{disk(7)}) \bullet_g K_{line90(71)}$$

A *white line* is composed of white , i.e. bright , vertical rectangle region , so it can be extracted from a white top-hat operation .

$$T_w(x) = |S_w(x) - S_w(x) \circ_g K_{line0(71)}|_{\theta_2}$$

where  $\theta_2 = 50$ .

Eliminating the small regions of  $T_w(x)$  ,  $T_{white}(x)$  can be obtained. Examples of  $G_o(x)$  , desired image and  $T_{white}(x)$  are shown in Fig. 7 , Fig. 8 and Fig. 9 respectively.

#### 5 Joint Detection

Since a *joint* is made of a kind of metal , it has smooth surface and can be detected by extracting

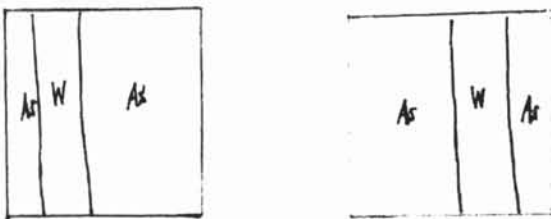


Figure 8: Desired image(*white line*)

flat regions. *Canny* edge detecting operator is used here to extract such regions.

$$C_j(x) = ((canny(G_o(x)))^c \circ K_{disk(9)}) \ominus K_{square(3)}$$

A *joint* region is broad enough to contacts to at least two image ends and wider than a quarter of the horizontal dimension of the image . Eliminating regions which are not satisfied both of these two conditions from  $C_j(x)$  , we can obtain  $E_j(x)$ . Final detecting result of *joint* is obtained after a dilation operation.

$$D_{joint}(x) = C_j(x) \oplus K_{square(3)}$$

Examples of  $G_o(x)$  , desired image and  $D_{joint}(x)$  are shown in Fig. 10 , Fig. 11 and Fig. 12 respectively.

#### 6 Manhole Detection

A *manhole* is a disk with rugged surface. A *manhole* has round shape , so we first extract round shape components. We use a black top-hat operation with disk shape structure element to extract that components.

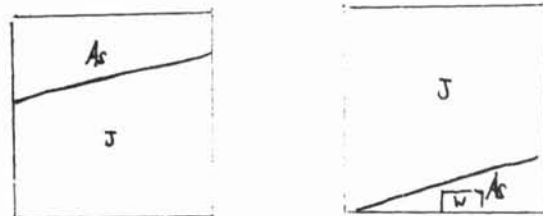


Figure 11: Desired image(*joint*)



Figure 12:  $D_{joint}$

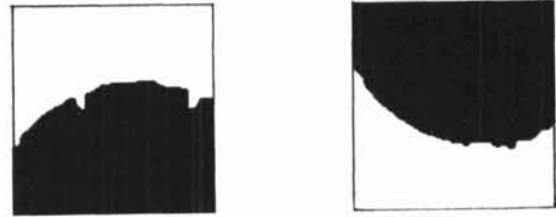


Figure 15:  $M_{manhole}$

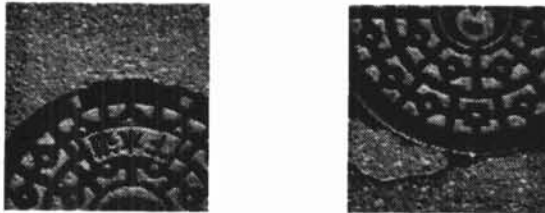


Figure 13:  $G_o(x)(manhole)$

$$T_m(x) = |G_o(x) \bullet_g K_{disk(31)} - G_o(x)|_{\theta_3}$$

where  $\theta_3 = 120$ . Because a *manhole* is composed of black regions, a masking operation is made on  $T_m(x)$  with the thresholded input image.

$$A_m(x) = T_m(x) \cap |G_o(x)|_{\theta_4}$$

where  $\theta_4 = 40$ . Eliminating the too small regions as a component of *manhole* from  $A_m(x)$ , then also eliminate the regions which include no hole. This is because the ruggedness of the surface makes some holes in the *manhole* components. Now we can obtain a result image  $M_{manhole}(x)$ . Examples of  $G_o(x)$ , desired image and  $M_{manhole}(x)$  are shown in Fig. 13, Fig. 14 and Fig. 15 respectively.

## 7 Experimental Results

We have 319 of road surface images as the test images, which are attached the interpretation results of the images via a expert. There exists 105 of *crack* images, 44 of *whiteline* images, 9 of *joint* images and 6 of *manhole* images among them. Each image

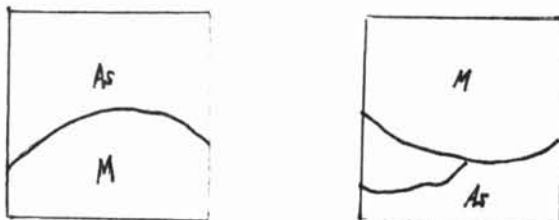


Figure 14: Desired image(*manhole*)

Table 1: The experimental results of crack and structural objects detection.

original	correct	false detection	correct ratio
<i>crack</i> (105)	97/105	15/214	92.8%(293/319)
<i>joint</i> (9)	9/9	3/310	99.1%(316/319)
<i>whiteline</i> (44)	40/44	0/275	91.0%(315/319)
<i>manhole</i> (6)	6/6	0/313	100%(319/319)

is processed by the four kind of detection processes simultaneously. The experimental results are shown in table 1.

## 8 Conclusion

A morphological method to detect *crack*, *whiteline*, *joint* and *manhole* of the road surface image is proposed in this paper. Although the proposed method requires the setting of some parameters, it is robust and high performance for detecting vague objects in the noisy road surface image.

## References

- [1] N. Tanaka, K. Uematsu, "A Crack Detection Method in Road Surface Images Using Morphology", IAPR Workshop on Machine Vision Applications '98, Nov. 1998, pp.154-157.
- [2] H. Talbot, "A Morphological Algorithm for Linear Segment Detection", Mathematical Morphology and its Applications to Image and Signal Processing, Kluwer Academic Pub. 1996.
- [3] R.M. Haralick, S.R. Sternberg, and Zhang, "Image analysis using mathematical morphology", IEEE Trans, PAMI, Vol.9, No.4, July 1987, pp.532-550.
- [4] R.M. Haralick, "Computer and Robot Vision", Addison Wesley, 1992.
- [5] J. Serra, "A nalysis and Mathematical Morphology", Academic Press, 1982.